



## Artificial Rabbits Optimization Based Optimal Allocation of Solar Photovoltaic Systems and Passive Power Filters in Radial Distribution Network for Power Quality Improvement

Chegudi Ranga Rao<sup>1,2\*</sup>

Ramadoss Balamurugan<sup>2</sup>

RamaKoteswaraRao Alla<sup>1</sup>

<sup>1</sup>Department of Electrical and Electronics Engineering, RVR & JC College of Engineering, Guntur, Andhra Pradesh-522019, India

<sup>2</sup>Department of Electrical Engineering, Annamalai University, Annamalai Nagar, Chidambaram, Tamilnadu-608002 India

\* Corresponding author's Email: rangarao.chegudi@gmail.com

---

**Abstract:** This paper presents an artificial rabbits optimization (ARO) based optimization methodology for the optimal location and rating of solar photovoltaic systems (SPVs) and passive power filters (PPFs) to mitigate the effects of non-fundamental frequencies due to the presence of non-linear and static loads in radial distribution networks (RDNs). The basic components of the distribution network are modelled for decoupled harmonic power flow (DHPF). The performance of RDN and harmonic levels is evaluated using DHPF. A multi-objective function using real power distribution loss (RPDL), voltage deviation index (VDI), total harmonic distortions in voltage (THDv), and current (THDi) is formulated by considering different equal and unequal planning and operational constraints. The effectiveness of the proposed methodology is evaluated on IEEE 33-bus RDN. Also, the computational efficiency of ARO is compared with other recent meta-heuristic approaches, namely the coyote optimization algorithm (COA), the butterfly optimization algorithm (BOA), the future search algorithm (FSA), and the pathfinder algorithm (PFA). The comparative analysis has highlighted the superiority of ARO in terms of global optima over the other compared algorithms. The reactive power losses and AVDI are reduced to 72.7865 kW, 50.6519 kW, and 0.0214 from 210.11 kW, 143.03 kVAr, and 0.0637, respectively. Also, integration of SPVs and single-tuned PPFs at optimal locations with appropriate sizes results in significantly improving the RDN power quality and performance significantly. The maximum in the entire network is observed at 5.21% of the fundamental frequency at bus-13. As per the IEEE 519 standards, it is required to maintain less than 5% and it is reduced to 3.98% with optimal PPF integration by the proposed method.

**Keywords:** Artificial rabbits optimization, Decoupled harmonic power flow, Passive power filters, Power quality, Harmonics, Radial distribution network, Solar photovoltaic systems.

---

### 1. Introduction

In recent years, the use of renewable energy (RE) [1] and the adoption of electric vehicles (EVs) [2] in the energy and transportation sectors have greatly expanded throughout the world in consideration of global warming and sustainability [3]. The stochastic and intermittent character of these technologies, however, results in a number of common operational and control problems in distribution systems [4]. Power imbalances, high distribution losses, uneven voltage profiles, lower voltage stability and reliability

margins, etc. are caused by improper locations, sizes, and their unpredictably high degrees of penetration. Contrarily, a variety of non-linear loads and their unpredictable loading profiles are a major cause of harmonics and poor power quality (PQ) problems. The main types of classified loads in distribution systems, such as residential, commercial, industrial, agricultural, and municipal loads, are very sensitive to changes in voltage and frequency when power electronics-based converters are used. As a result, a lot of research has been focused on finding the best ways to allocate distribution generation (DG),

capacitor banks (CBs), custom power devices (CPDs), energy storage systems (ESSs), and network reconfiguration (NR), among other technologies, to improve the techno-economic-environmental performance of modern distribution systems [5, 6]. The most commonly used methods for resolving PQ issues include distribution static synchronous compensator (DSTATCOM), active power filters (APF), passive power filters (PPF), active power conditioner (APC), unified power quality conditioner (UPQC), and dynamic voltage restorer (DVR) [7]. In addition to renewable energy (RE) sources [8], hybridization of the aforementioned methods with new trends like grid-scale ESSs [9] and electric vehicles [10] is receiving a lot of interest at the moment. To maintain the harmonic-related operational features in line with IEEE-519 standards, it is still a potential problem to identify the location and size of any form of PQ device(s) in distribution systems [11].

Due to their radiality configuration with low R/X distribution lines, metaheuristic approaches for solving the optimal allocation of PQ devices in radial distribution systems (RDSs) have received a lot of attention in recent work. A genetic algorithm (GA) is used in [12] to allocate PPFs in RDSs while considering multiple objectives such as loss reduction and PPF investment cost. In [13], different configured single-tuned passive filters are optimally located with their proper sizes in unbalanced distribution systems for THD mitigation using GA. In [14], the lion algorithm (LA) and crow search algorithm (CSA) are hybridised for optimally allocating UPQCs in RDSs considering loss reduction, VSI maximization, and reduction of the cost of UPQC. Under load tap changer (ULTC) and reactive power controls of photovoltaic-DGs are optimally tuned using phasor particle swarm optimization (PPSO) and gravitational search algorithm (GSA) towards Volt/controls in RDSs. In [16], the strength Pareto evolutionary algorithm 2 (SPEA-II) is used for simultaneous allocation of CBs, single-tuned and high-pass passive filters, considering optimization of energy loss cost, installation cost, and THD. In [17], Harris-Hawks optimization (HHO) is used to find the best way to integrate resonance-free C-type harmonic filters to reduce harmonic overloading and, as a result, a number of PQ problems in distribution networks with loads that change with voltage and frequency. In [18], an improved discrete firefly algorithm (IDFA) with GA is proposed for optimally integrating APCs in RDSs for loss minimization, voltage profile improvement, THD, and investment cost. In [19], enhanced bacterial foraging optimization (EBFO) is

proposed for identifying the location and sizes of different kinds of DFACTS/CPDs for loss reduction, load balancing, and voltage deviation index. [20, 21] present a modified adaptive binary imperialist competitive algorithm (MABICA) and a basic imperialist competitive algorithm (ICA) with fuzzy logic for allocating APFs while taking techno-economic goals into account. In [22], the grey wolf optimizer (GWO) is used for optimal allocation of multiple APFs for solving PQ issues due to non-linear loads. In [23], a fuzzy-lightning search algorithm (FLSA) is proposed for optimal allocation of DSTATCOM in PV integrated distribution systems for loss reduction, voltage profile improvement, and voltage stability enhancement. Also like this are the improved bacterial foraging search algorithm (IBFA) [24], the gravitational search algorithm (GSA) [25], the imperialist competitive algorithm (ICA) [26], the rooted tree optimization (RTO) [27], the different types of PSOs [28], the bat algorithm (BA) [29], and the cuckoo search algorithm (CSA) [30].

According to this work, optimal location and sizing of PQ devices helps handle RE uncertainty and non-linear loads in distribution systems. The NFL theorem states that no single optimization algorithm can solve all optimization problems [31]. Researchers are still inspired to develop new algorithms or hybrid algorithms. ARO was introduced in 2022 by inspiring rabbits' social and survival behaviours [32]. This paper used ARO to optimise SPV system allocation by minimising loss and voltage deviation index. In the second stage, APFs are analysed and compared for handling PQ issues under harmonic current sources by BESS. In both stages, ARO's computational efficiency is compared to literature and metaheuristic algorithms. Different scenarios are simulated on the IEEE 33-bus RDN. The rest of the paper is organised as follows. In section 2, mathematical modelling of distribution and SPV systems, and section 3, the proposed multi-objective function and different constraints are explained. Section 4 discusses ARO modelling. Section 5 discusses 33-bus RDN simulation results. Section 6 summarises the paper's contributions and research findings.

## 2. Mathematical modelling of concepts

In this section, the mathematical modelling of different components associated with distribution system is explained as suitable for decoupled harmonic power flow [33].

## 2.1 Modelling of components

The basic components of harmonic distribution system such as branch admittances  $y_{pq(h)}$ , linear loads  $y_{d,k(h)}$ , non-linear loads  $\bar{y}_{d,k(h)}$ , shunt capacitors  $y_{sh,k(h)}$ , and shunt passive filters  $y_{fl,k(h)}$ , are modelled in admittance form considering harmonic frequencies as given by [22],

$$y_{pq(h)} = \frac{1}{R_{pq} + j2\pi f^{(h)}L_{pq}}, pq \in 1:n_{br} \quad (1)$$

$$y_{d,k(h)} = \frac{P_{d,k}}{|V_{k(1)}|^2} - j \frac{Q_{d,k}}{f^{(h)}|V_{k(1)}|^2}, pq \in 1:n_b \quad (2)$$

$$I_{d,k(1)} = \left( \frac{\bar{P}_{d,k} + j\bar{Q}_{d,k}}{|V_{k(1)}|} \right)^*, k \in 1:n_{bus} \quad (3)$$

$$\bar{I}_{d,k(h)} = k^{(h)}I_{d,k(1)}, k \in 1:n_{bus} \quad (4)$$

$$y_{sh,k(h)} = f^{(h)}y_{sh,k(1)}, k \in 1:n_{sh} \quad (5)$$

$$y_{fl,k(h)} = \frac{1}{Z_{fl(h)}}, k \in 1:n_{fl} \quad (6)$$

where  $R_{pq}$  and  $L_{pq}$  are the resistance and inductances of a branch connected between buses  $p$  and  $q$ , respectively;  $f^{(h)}$  is the harmonic order,  $P_{d,k}$  and  $Q_{d,k}$  are the real and reactive components of linear load at bus- $k$ , respectively,  $\bar{P}_{d,k}$  and  $\bar{Q}_{d,k}$  are the real and reactive components of non-linear load at bus- $k$ , respectively,  $y_{sh,k(1)}$  is the shunt capacitive admittance at fundamental frequency,  $Z_{fl(h)}$  is the impedance of shunt filter at bus- $k$ ,  $I_{d,k(1)}$  and  $\bar{I}_{d,k(h)}$  are the non-linear load currents at fundamental frequency and  $h$ th harmonic order at bus- $k$ ,  $k^{(h)}$  is the ratio of the  $h$ th harmonic current to fundamental current,  $n_{br}$ ,  $n_b$ ,  $n_{sh}$  and  $n_{fl}$  are the number of branches, number buses, number of shunt capacitors, number of filters in the network, respectively.

## 2.2 Decoupled harmonic power flow

By determining the bus admittance matrix  $Y_{bus(h)}$ , and current injection vector  $I_{bus(h)}$  at the  $h$ th harmonic order, the bus voltage vector  $V_{bus(h)}$  can be determined by,

$$V_{bus(h)} = [Y_{bus(h)}]^{-1} I_{bus(h)} \quad (7)$$

$$I_{bus(h)} = [I_1(h), I_2(h), \dots, I_{nb(h)}]^T \quad (8)$$

$$V_{bus(h)} = [V_1(h), V_2(h), \dots, V_{nb(h)}]^T \quad (9)$$

where  $I_{i(h)}$  and  $V_{i(h)}$  are the injection current and voltage at bus- $i$ , respectively. The diagonal  $Y_{pp(h)}$  and off-diagonal elements  $Y_{pq(h)}$  in  $Y_{bus(h)}$  are determined by Eq. (10) and (11), respectively,

$$Y_{pp(h)} = \sum_p y_{pq(h)} + y_{d,p(h)} + y_{sh,p(h)} + y_{fl,p(h)}, p \in 1:n_b \quad (10)$$

$$Y_{pq(h)} = Y_{qp(h)} = -y_{pq(h)}, pq \in 1:n_{br} \quad (11)$$

By using harmonic bus voltages determined using Eq. (7), the RMS and  $THD_V$  levels can be evaluated. The total active power distribution losses  $P_{loss(h)}$  can be evaluated by,

$$P_{loss(h)} = \sum_{h=1}^H \sum_{pq=1}^{n_{br}} \left\{ R_{pq} (|V_p(h)| - |V_q(h)|) \left| |Y_{pq(h)}| \right| \right\}^2 \quad (12)$$

## 2.3 Solar photovoltaic system

The energy generation from a SPV system  $P_{SPV(t)}$  is dependent on climatic conditions of a location and its various design parameters. It can be estimated mathematically by,

$$P_{SPV(t)} = SPV_r \times \mu_d \times \frac{G(t)}{G_r} [1 + \tau_t(T_c - T_r)] \quad (13)$$

$$T_c = T_a + G(t) \times \left( \frac{NOCT - 20}{0.8} \right) \quad (14)$$

where  $\tau_t = -3.7 \times 10^{-3}$  ( $1/^\circ\text{C}$ ) for poly-crystalline and mono-silicon panels.  $T_c$ ,  $T_a$ ,  $T_r$  and  $NOCT$  are the cell, ambient, reference/STC and, normal operating cell temperatures in  $^\circ\text{C}$ , respectively,  $G(t)$  and  $G_r$  are the actual and reference radiation at a location, respectively;  $SPV_r$  and  $\mu_d$  are the SPV rated capacity and degrading efficiency of the panels, respectively.

In general, SPV system connects with grid directly via DC-AC converter which operates at unity power factor. Thus, the reactive power injection by SPV system is zero. Since, the power generation by SPV systems are highly intermittency in nature, this research assumes that they are first integrated to battery energy storage system (BESS) via DC-DC converter and later, BESS is integrated with grid via DC-AC inverter which can capable to operate at different power factors. Hence, Eq. (15) and Eq. (16) are given for real and reactive power injections by SPV system at a bus- $k$ , respectively.

$$\bar{P}_{d,k} = P_{d,k(0)} - P_{SPV(t)} \quad (15)$$

$$\bar{Q}_{d,k} = Q_{d,k(0)} - P_{SPV(t)} \times \tan(\phi_k) \quad (16)$$

where  $P_{d,k(0)}$  and  $Q_{d,k(0)}$  are the real and reactive powers of bus- $k$  before SPV integration, respectively;  $\bar{P}_{d,k}$  and  $\bar{Q}_{d,k}$  are the real and reactive powers of bus- $k$  after SPV integration, respectively;  $pf_k = \cos(\phi_k)$  is the inverter's operating power factor at bus- $k$ .

By this modelling, SPV system with BESS can be treated as dispatchable generator in the load flow studies.

### 3. Problem formulation

In this paper, four major objective functions are considered for multi-objective function.

The first objective is to minimize total real power distribution losses, given by,

$$of_1 = \min(P_{loss}(h)) \quad (17)$$

where  $P_{loss}(h)$  is the real power loss at time- $t$  and frequency- $h$ ,  $T$  and  $H$  are time duration and maximum harmonic order under consideration, respectively.

The second objective is to minimize average voltage deviation index (AVDI), given by,

$$of_2 = \min \left\{ \frac{1}{\sqrt{n_b}} \sqrt{\sum_{k=1}^{n_b} \left( \frac{(|V_{k(h)}| - |V_{k(1)}|)}{|V_{k(1)}|} \right)^2} \right\} \quad (18)$$

The third and fourth objectives are to maximize power quality by minimizing both  $THD_v$  and  $THD_i$  as given by [22],

$$of_3 = \min \left\{ \max_{k \in n_b} \left( \frac{1}{|V_{k(1)}|} \right) \sqrt{\sum_{h=2}^H (|V_{k(h)}|)^2} \right\} \quad (19)$$

$$of_4 = \min \left\{ \max_{k \in n_b} \left( \frac{1}{|I_{k(1)}|} \right) \sqrt{\sum_{h=2}^H (|I_{k(h)}|)^2} \right\} \quad (20)$$

where  $|V_{k(h)}|$  and  $|V_{k(1)}|$  are the voltage magnitudes of bus- $k$  at fundamental and frequency- $h$ , respectively,  $|I_{k(h)}|$  and  $|I_{k(1)}|$  are the current magnitudes of bus- $k$  at fundamental and frequency- $h$ , respectively.

The bus voltages, SPV capacity, filter capacity,  $THD_v$  and  $THD_i$  limits are considered, as given by,

$$|V_{rms(k)}^{min}| \leq \left( \sqrt{\sum_{h=2}^H (|V_{k(h)}|)^2} \right) \leq |V_{rms(k)}^{max}| \quad (21)$$

$$SPV_r^{min} \leq SPV_r \leq SPV_r^{max} \quad (22)$$

$$S_{fl}^{min} \leq S_{fl(k)} \leq S_{fl}^{max} \quad (23)$$

$$THD_{v(k)} \leq THD_v^{max} \quad (24)$$

$$THD_{i(k)} \leq THD_i^{max} \quad (25)$$

where min and max denotes the minimum and maximum limits of the variable, respectively;  $THD_{v(k)}$  and  $THD_{i(k)}$  are the distortion in voltage, current at bus- $k$ , respectively.

### 4. Artificial rabbits optimization

In order to survive, rabbits in nature use detour foraging and random concealment techniques, which they use during the exploration and exploitation phases of their life cycle [32]. The mathematical modelling of these tactics in artificial rabbits optimization (ARO) is provided in this section.

#### 4.1 Exploration phase

When searching for food, rabbits don't focus on what is nearby and instead look in the distance. When they only consume grass from areas other than their home range, this is known as detour foraging. Consider a swarm of bunnies, each with its own territory filled with grass and its burrows, and visiting each other at random to eat. In areas with an abundance of food, rabbits search for it. Each search individual tends to update its position toward a random swarm member and contribute a disturbance when an ARO is looking for food. Model for rabbit foraging diversion proposed:

$$\bar{A}_{pi}^{k+1} = \bar{A}_{pi}^k + k_r \times (A_{pi}^k - A_{pj}^k) + \text{round} \\ (0.5 \times (0.05 + r_1)) \times k_{r1}, \quad i, j = 1: n_p, j \neq i \quad (26)$$

$$k_r = a_L \times \rho_{(m)} \quad (27)$$

$$a_L = \left( e - e^{\left( k - \frac{1}{k_{max}} \right)^2} \right) \times \sin(2\pi r_2) \quad (28)$$

$$\rho_{(m)} = \begin{cases} 1 & \text{if } m == x(y), m = 1: n_d \& \\ 0 & \text{else} \end{cases} \quad y = 1, 2, \dots, (r_3 n_d) \quad (29)$$

$$x = \text{randperm}(n_d) \& k_{r1} \sim N(0,1) \quad (30)$$

where  $\bar{A}_{pi}^{k+1}$  and  $A_{pi}^k$  are the  $i$ th rabbit at iteration  $(k+1)$  and  $k$ , respectively;  $n_p$  and  $n_d$  are the number of

rabbits (population) and number of burrows (dimension), respectively;  $k_{max}$  is the number of maximum iterations,  $r_1, r_2$  and  $r_3$  are the random numbers with uniform distribution and  $k_{r1}$  is a normal distribution random number;  $a_L$  is running length of rabbits for dynamic behaviour of rabbits, which results for exploration phase with longer step or exploitation phase with shorter step size,  $k_r$  demonstrates the running characteristics of a rabbit,  $\rho_{(m)}$  is a mapping vector that helps the algorithm randomly alter search individuals' foraging behaviour.

Based on their positions, Eq. (26) shows that searchers look for food in a random way. This lets a rabbit go to the homes of other rabbits. This tendency of rabbits to visit other nests instead of their own helps to explore and makes sure that the ARO algorithm can search all over the world.

## 4.2 Exploitation phase

Rabbits construct  $n_p$  burrows around their nests as a means of child protection. In ARO, the rabbit always excavates tunnels around itself in all directions. Then, in order to reduce its chances of being eaten, it randomly chooses a hole to hide in. Eq. (31) provides the random concealment method,

$$\bar{A}_{pi}^{k+1} = A_{pi}^k + k_r \times (r_4 B_{ij}^k - A_{pj}^k) \quad i = 1:n_p \quad (31)$$

Here,  $B_{pi}^k$  is the burrow chosen at random for shielding from its  $n_d$  burrows, and defined by,

$$B_{pi}^k = A_{pi}^k + N_r \gamma A_{pi}^k, \quad i = 1:n_p, m = 1:n_d \quad (32)$$

$$N_r = r_4 \times \left( \frac{k_{max} - k + 1}{k_{max}} \right) \quad (33)$$

$$\rho_{(m)} = \begin{cases} 1 & \text{if } m == [r_5 \times n_d] \\ 0 & \text{else} \end{cases}, \quad m = 1:n_d \quad (34)$$

where  $r_4$  and  $r_5$  are the uniformly distributed random numbers between 0 and 1, respectively.

At this stage, ARO changes the global position and solution at this point using the detour foraging or hiding behaviour defined by,

$$A_{pi}^{k+1} = \begin{cases} A_{pi}^k & f(A_{pi}^k) \leq f(\bar{A}_{pi}^{k+1}) \\ \bar{A}_{pi}^{k+1} & f(A_{pi}^k) > f(\bar{A}_{pi}^{k+1}) \end{cases} \quad (35)$$

This equation states that if the fitness of the  $i$ th rabbit's position is greater than the fitness of the current position, the rabbit will abandon the current

position and remain at the candidate position generated by either Eq. (26) or Eq. (31).

## 4.3 Switching between phases

In ARO, rabbits forage at the start of iterations and hide at the end. Detours make foraging harder. This search method uses rabbit energy, which will shrink over time. Exploration to exploitation phases requires an energy factor model. The energy factor  $E_{f(k)}$  in ARO is defined by,

$$E_{f(k)} = 4 \times \ln\left(\frac{1}{r_6}\right) \times \left(1 - \frac{1}{k_{max}}\right) \quad (36)$$

If a rabbit has a high energy factor, it can forage in a new region. Low energy makes a rabbit less active and needing to hide. When  $E_{f(k)} > 1$ , a rabbit will detour browse in other rabbits' territories and when  $E_{f(k)} \leq 1$ , a rabbit will randomly use its own burrows.

## 5. Results and discussion

The proposed ARO for the optimal allocation of SPV systems and PPFs is evaluated on IEEE 33-bus RDN. Simulations are performed for two different scenarios. In scenario 1, optimal allocation of SPV systems is presented. In scenario 2, optimal allocation of PPFs is presented.

### 5.1 Optimal allocation of SPV systems

It serves totally 3715 kW and 2300 kVAr, real and reactive power loads, respectively. The operating voltage of the network is 12.66 kV. By implementing the DHLF at fundamental harmonic order using ETAP software, the distribution losses are determined as 210.9976 Kw and 143.0325 kVAr, respectively. The network observed for lowest voltage magnitude and it is registered as 0.9038 p.u. at bus-18. The AVDI of the network is estimated as 0.0637 p.u. The results of ETAP software are given in Fig. 1. This operating condition is considered as base case.

In this first scenario, the network is assumed as harmonics-free network and the SPV systems are optimally integrated to minimize simultaneously real power loss and AVDI, i.e.,  $\min(of_1 + of_2)$ . Also, the inverter operating power factor of SPV systems' is considered as unity and thus, the reactive power injection by SPV systems are zero.

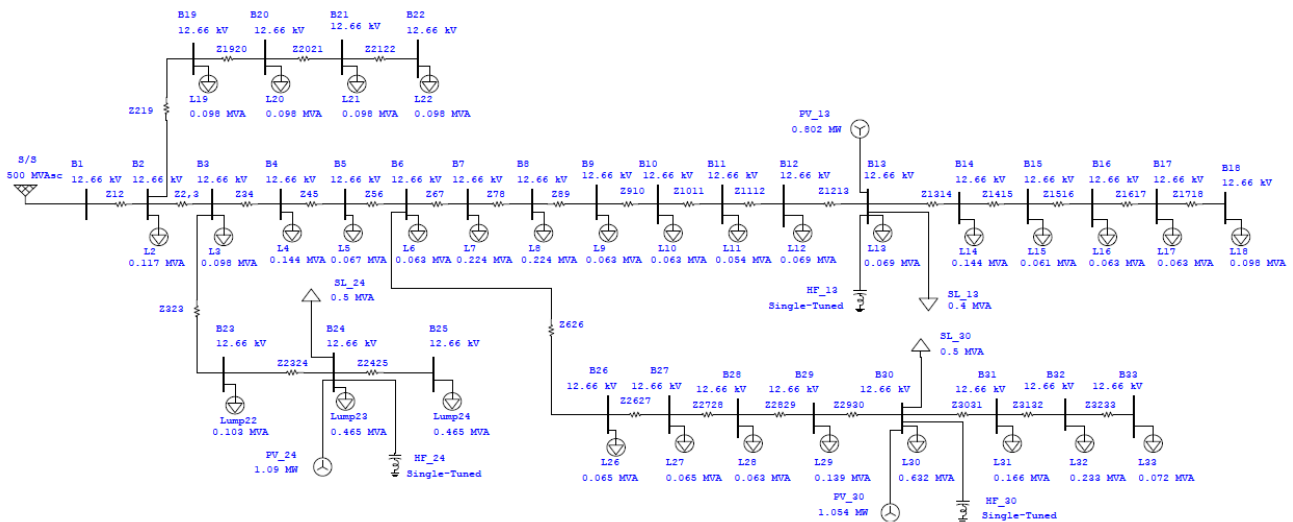


Figure. 1 Network model in ETAP software

Table 1. Optimal locations and sizes of SPV systems by different algorithms and comparison of their convergence characteristics over 50 independent runs

| Algorithm  | SPV Locations |           |           | SPV Sizes (kW)  |                |                 | Target Value   |                |                |               |
|------------|---------------|-----------|-----------|-----------------|----------------|-----------------|----------------|----------------|----------------|---------------|
|            | Best          | Worst     | Median    | Best            | Worst          | Median          | Best           | Worst          | Median         | Std.          |
| COA        | 24            | 13        | 30        | 1075.306        | 811.245        | 1046.969        | 72.8152        | <b>85.7251</b> | 76.2533        | <b>2.8190</b> |
| BOA        | 14            | 6         | 31        | 646.910         | 1189.675       | 686.418         | 78.4740        | 113.9889       | 78.5063        | 6.3852        |
| FSA        | 30            | 3         | 14        | 1008.547        | 1711.595       | 746.421         | 77.9144        | 117.8797       | 77.9145        | 5.9028        |
| PFA        | 12            | 24        | 30        | 895.987         | 1074.630       | 1016.916        | 73.3646        | 110.2622       | 75.2847        | 9.6621        |
| <b>ARO</b> | <b>30</b>     | <b>13</b> | <b>24</b> | <b>1053.585</b> | <b>802.441</b> | <b>1089.637</b> | <b>72.8079</b> | 97.2630        | <b>73.3946</b> | 4.3376        |

Table 2. Comparison of ARO with literature works

| Reference   | SPV Locations          |                          |           | SPV Sizes (kW)  |                |                 | Network Performance |                |               |
|-------------|------------------------|--------------------------|-----------|-----------------|----------------|-----------------|---------------------|----------------|---------------|
|             | P <sub>loss</sub> (kW) | Q <sub>loss</sub> (kVar) | AVDI      |                 |                |                 |                     |                |               |
| Base        | -                      | -                        | -         | -               | -              | -               | 210.9976            | 143.0325       | 0.0637        |
| MOIDSA [37] | 30                     | 13                       | 25        | 968.7           | 800            | 1036.3          | 74.2564             | 51.6199        | 0.0229        |
| PSO [36]    | 14                     | 24                       | 29        | 691             | 986.1          | 1277.3          | 74.0977             | 51.8412        | 0.0213        |
| SKHA [34]   | 24                     | 14                       | 30        | 914.98          | 750.199        | 1142.405        | 73.2966             | 50.9849        | 0.0214        |
| MRFO [39]   | 13                     | 24                       | 30        | 788             | 1017           | 1035            | 72.9008             | 50.6596        | 0.0223        |
| PO [35]     | 13                     | 24                       | 30        | 800             | 1069           | 1064            | 72.7944             | 50.6541        | 0.0214        |
| HGWO [38]   | 13                     | 24                       | 30        | 802             | 1090           | 1054            | 72.7865             | 50.6519        | 0.0214        |
| <b>ARO</b>  | <b>30</b>              | <b>13</b>                | <b>24</b> | <b>1053.585</b> | <b>802.441</b> | <b>1089.637</b> | <b>72.7865</b>      | <b>50.6519</b> | <b>0.0214</b> |

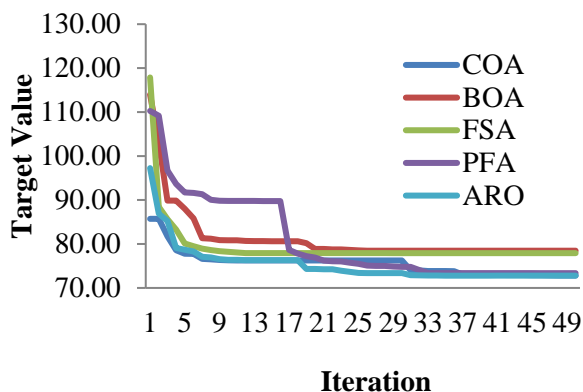


Figure. 2 Convergence characteristics of different algorithms SPV systems allocation

In order to find the optimal locations for SPV systems, all buses except sub-station bus are considered as search space. The maximum limit for SPV system capacities is considered as total network real power load i.e., 3715 kW. However, the summation of all SPV system capacities should not be more than total load demand. Considering number maximum iterations and population as 50 and 30 respectively, ARO is implemented for finding the optimal locations and sizes of SPV systems. The optimal results provided by ARO and other algorithms are given in Table 1. In order to validate the computational efficiency of ARO, 50 independent runs are performed and the comparison of statistical

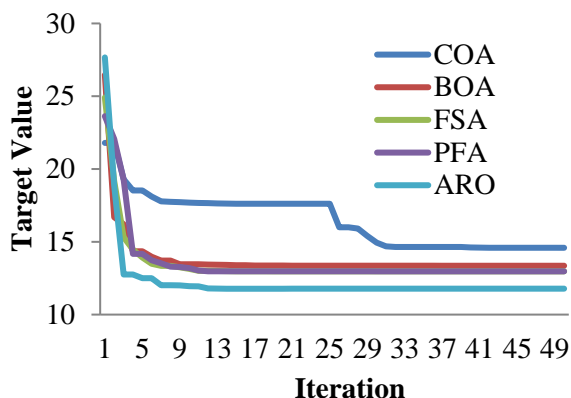


Figure. 3 Convergence characteristics of different algorithms for PPFs allocation

parameters is also given in Table 1. Also, the computational efficiency of ARO is compared with other recent meta-heuristic approaches, namely the coyote optimization algorithm (COA), the butterfly optimization algorithm (BOA), the future search algorithm (FSA), and the pathfinder algorithm (PFA). As per the overall target value and median values, ARO is performed highly competitive with COA. With least worst and std. values, COA is stood in the 2nd place in comparison. The convergence characteristics of all algorithms are given in Fig. 2.

The optimal locations and SPV systems by ARO are as follows: locations bus 30, 13 and 24 and capacities of 1053.585 kW, 802.441 kW, and 1089.637 kW, respectively. By having these SPV systems, the network performance is improved as follows: the distribution losses are determined as 72.7865 kW ( $of_1$ ) and 50.6519 kVAr, respectively. The network observed for lowest voltage magnitude and it is registered as 0.9687 p.u. at bus-33. The AVDI ( $of_2$ ) of the network is estimated as 0.0214 p.u.

In comparison to the base case, both  $of_1$  and  $of_2$  are reduced significantly and the network performance is said to be improved. The losses are reduced and voltage profile is improved significantly. On the other hand, the optimal results of ARO are compared with literature works and the comparison is given in Table 2. From the results, ARO results are superior in terms of network performance than MOIDSA [4], PSO [3], SKHA [1], MRFO [6], PO [2] and HGWO [5]. However, the results obtained by ARO are highly competitive with HGWO. From this comparison, ARO is said to be global optimization algorithm with high accuracy.

However, as per NFL [31], the performance of ARO is still needed to compare with recent meta-heuristics such as fixed step average and subtraction based optimizer (FS-ASBO) [40], stochastic komodo algorithm (SKA) [41], mixed leader based optimizer

(MLBO) [42], three influential members based optimizer (TIMBO) [43], random selected leader based optimizer (RSLBO) [44], puzzle optimization algorithm (POA) [45], and ring toss game-based optimization algorithm (RTGBO) [46]. This can be treated as one of the future scopes of this work.

## 5.2 Optimal allocation of PPFs systems

In this second scenario, PPFs are optimally designed and integrated at each SPV location. BESS are treated as static loads for harmonic sources. In this scenario, the overall objective function is to minimize all proposed objectives simultaneously. The optimal locations obtained for SPV systems by ARO are buses 13, 24 and 30 and thus they are considered as harmonic current sources due to the presence of DC-DC converters and DC-AC inverters with BESS.

In first case, for creating harmonics in the network, three BESSs of  $(0.392+j0.08)$ ,  $(0.49+ j0.099)$  and  $(0.49+j0.099)$  in MVA are considered at buses 13, 24 and 30, respectively. By modelling BESS as static loads in ETAP software, the harmonic load flow analysis is performed. Typical IEEE 6 Pulse 1 model is considered as current harmonic source for all static loads. For integrating single-tuned filters, the convergence characteristics are given in Fig. 3 and comparison of  $THD_v$  for different cases are given in Fig. 4.

The optimized PPF parameters at buses 24 and 30 are as follows: kVAR = 99.499, C = 1.976  $\mu$ F, X = 64.6332, and Q-factor = 100. Similarly, at bus 13 are follows: kVAR = 79.599, C = 1.581  $\mu$ F, X = 80.5415, and Q-factor = 100.

## 6. Conclusion

Radial distribution networks (RDNs) perform poorly due to radiality and non-linear loads. This research proposes Artificial rabbit optimization (ARO) for the best position and rating of solar PV systems (SPVs) and passive power filters (PPFs) to mitigate non-fundamental frequencies in RDN. Decoupled harmonic power flow (DHPF) is modelled on distribution network components. DHPF evaluates RDN and harmonics. A proposed approach was tested on the IEEE 33-bus RDN. ARO's computing efficiency is compared to ETAP 12.6.5. Comparative analysis indicates ARO's global optimality advantage. SPVs and single-tuned PPFs improve RDN power quality and performance. Real power losses, reactive power losses, and VDI decline from 210.11 kW, 143.03 kVAr, and 0.0637 to 72.7865 kW, 50.6519 kW, and 0.014. Also, at bus-13,

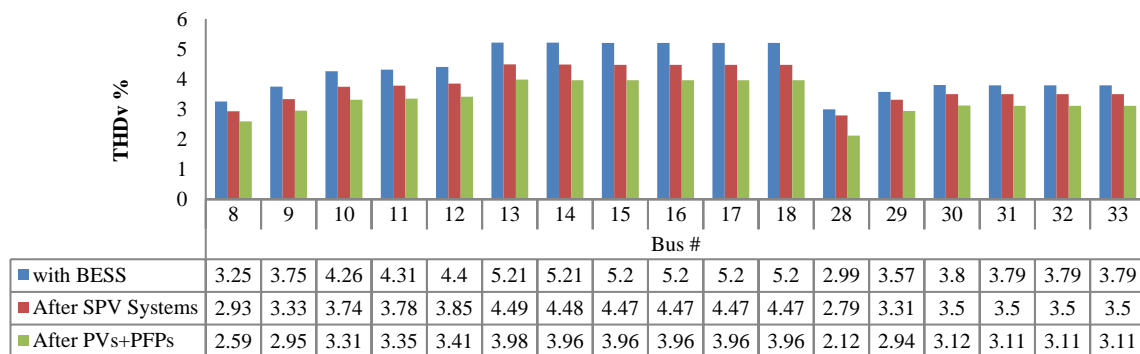


Figure. 4 Comparison of THDv for different cases

the fundamental frequency has the greatest THDv of 5.21%. The IEEE 519 standards require less than 5%, while the proposed approach reduces it to 3.98 % by integrating PPFs. From this, integrating SPVs and single-tuned PPFs in the proper positions and sizes improves RDN power quality and performance.

### Conflicts of interest

Authors declare that no conflicts of interest.

### Author Contributions

Chegudi RangaRao: Conceptualization, software, investigation, writing—original draft preparation, R Balamurugan and RamaKoteswaraRao Alla: validation, formal analysis, and supervision.

### References

- [1] I. Alotaibi, M. A. Abido, M. Khalid, and A. V. Savkin, "A comprehensive review of recent advances in smart grids: A sustainable future with renewable energy resources", *Energies*, Vol. 13, No. 23, p. 6269, 2020.
- [2] Z. Rezvani, J. Jansson, and J. Bodin, "Advances in consumer electric vehicle adoption research: A review and research agenda", *Transportation research part D: transport and environment*, Vol. 34, pp. 122-136, 2015.
- [3] L. M. Fonseca, J. P. Domingues, and A. M. Dima, "Mapping the sustainable development goals relationships", *Sustainability*, Vol. 12, No. 8, p. 3359, 2020.
- [4] M. S. Alam and S. A. Arefifar, "Energy management in power distribution systems: Review, classification, limitations and challenges", *IEEE Access*, Vol. 7, pp. 92979-93001, 2019.
- [5] V. A. Evangelopoulos, P. S. Georgilakis, and N. D. Hatziaargyriou, "Optimal operation of smart distribution networks: A review of models, methods and future research", *Electric Power Systems Research*, Vol. 140, pp. 95-106, 2016.
- [6] S. A. Kazmi, M. K. Shahzad, A. Z. Khan, and D. R. Shin, "Smart distribution networks: A review of modern distribution concepts from a planning perspective", *Energies*, Vol. 10, No. 4, p. 501, 2017.
- [7] O. P. Mahela and A. G. Shaik, "Topological aspects of power quality improvement techniques: A comprehensive overview", *Renewable and Sustainable Energy Reviews*, Vol. 58, pp. 1129-1142, 2016.
- [8] M. Bajaj and A. K. Singh, "Grid integrated renewable DG systems: A review of power quality challenges and state-of-the-art mitigation techniques", *International Journal of Energy Research*, Vol. 44, No. 1, pp. 26-69, 2020.
- [9] C. K. Das, O. Bass, G. Kothapalli, T. S. Mahmoud, and D Habibi, "Overview of energy storage systems in distribution networks: Placement, sizing, operation, and power quality", *Renewable and Sustainable Energy Reviews*, Vol. 91, pp. 1205-1230, 2018.
- [10] A. Ahmadi, A. Tavakoli, P. Jamborsalamati, N. Rezaei, M. R. Miveh, F. H. Gandoman, A. Heidari, and A. E. Nezhad, "Power quality improvement in smart grids using electric vehicles: a review", *IET Electrical Systems in Transportation*, Vol. 9, No. 2, pp. 53-64, 2019.
- [11] *IEEE recommended practices and requirements for harmonic control in electrical power systems*, IEEE Std. 519-1992, IEEE New York, 1993.
- [12] M. Milovanović, J. Radosavljević, D. Klimenta, and B Perović, "GA-based approach for optimal placement and sizing of passive power filters to reduce harmonics in distorted radial distribution systems", *Electrical Engineering*, Vol. 101, No. 3, pp. 787-803, 2019.
- [13] I. D. Melo, J. L. Pereira, A. M. Variz, and P. F. Ribeiro, "Allocation and sizing of single tuned passive filters in three-phase distribution



- systems for power quality improvement”, *Electric Power Systems Research*, Vol. 180, p. 106128, 2020.
- [14] K. Gaddala and P. S. Raju, “Merging lion with crow search algorithm for optimal location and sizing of UPQC in distribution network”, *Journal of Control, Automation and Electrical Systems*, Vol. 31, No. 2, pp. 377-392, 2020.
- [15] M. J. Milovanović and J. N. Radosavljević, “A Hybrid PPSOGSA Algorithm for Optimal Volt/VAr/THDv Control in Distorted Radial Distribution Systems”, *Applied Artificial Intelligence*, Vol. 35, No. 3, pp. 227-246, 2021.
- [16] H. D. Alves, “Power factor correction and harmonic filtering planning in electrical distribution network”, *Journal of Control, Automation and Electrical Systems*, Vol. 27, No. 4, pp. 441-451, 2016.
- [17] S. H. Aleem, A. F. Zobaa, M. E. Balci, and S. M. Ismael, “Harmonic overloading minimization of frequency-dependent components in harmonics polluted distribution systems using harris hawks optimization algorithm”, *IEEE Access*, Vol. 7, pp. 100824-100837, 2019.
- [18] M. Farhoodnea, A. Mohamed, H. Shareef, and H. Zayandehroodi, “Optimum placement of active power conditioner in distribution systems using improved discrete firefly algorithm for power quality enhancement”, *Applied Soft Computing*, Vol. 23, pp. 249-258, 2014.
- [19] M. Mohammadi, M. Montazeri, and S. Abasi, “Bacterial graphical user interface oriented by particle swarm optimization strategy for optimization of multiple type DFACTS for power quality enhancement in distribution system”, *Journal of Central South University*, Vol. 24, No. 3, pp. 569-588, 2017.
- [20] A. M. Far and A. AkbariForoud, “Cost-effective optimal allocation and sizing of active power filters using a new fuzzy-MABICA method”, *IETE Journal of Research*, Vol. 62, No. 3, pp. 307-322, 2016.
- [21] A. Moradifar and A. AkbariForoud, “A hybrid fuzzy DIAICA approach for cost-effective placement and sizing of APFs”, *IETE Technical Review*, Vol. 34, No. 5, pp. 579-589, 2017.
- [22] A. Lakum and V. Mahajan, “Optimal placement and sizing of multiple active power filters in radial distribution system using grey wolf optimizer in presence of nonlinear distributed generation”, *Electric Power Systems Research*, Vol. 173, pp. 281-290, 2019.
- [23] G. Isha and P. Jagatheeswari, “Optimal allocation of DSTATCOM and PV array in distribution system employing fuzzy-lightning search algorithm”, *Automatika*, Vol. 62, Nos. 3-4, pp. 339-352, 2021.
- [24] B. Khan, K. Redae, E. Gidey, O. P. Mahela, I. B. Taha, and M. G. Hussien, “Optimal integration of DSTATCOM using improved bacterial search algorithm for distribution network optimization”, *Alexandria Engineering Journal*, Vol. 61, No. 7, pp. 5539-5555, 2022.
- [25] A. K. Arya, A. Kumar, and S. Chanana, “Analysis of distribution system with D-STATCOM by gravitational search algorithm (GSA)”, *Journal of The Institution of Engineers (India): Series B*, Vol. 100, No. 3, pp. 207-215, 2019.
- [26] M. Sedighzadeh and A. E. Moarref, “The imperialist competitive algorithm for optimal multi-objective location and sizing of DSTATCOM in distribution systems considering loads uncertainty”, *INAE Letters*, Vol. 2, No. 3, pp. 83-95, 2017.
- [27] S. Sannigrahi and P. Acharjee, “Maximization of system benefits with the optimal placement of DG and DSTATCOM considering load variations”, *Procedia Computer Science*, Vol. 143, pp. 694-701, 2018.
- [28] M. Zellagui, A. Lasmari, S. Settoul, R. A. E. Sehiemy, C. Z. E. Bayeh, and R. Chenni, “Simultaneous allocation of photovoltaic DG and DSTATCOM for techno-economic and environmental benefits in electrical distribution systems at different loading conditions using novel hybrid optimization algorithms”, *International Transactions on Electrical Energy Systems*, Vol. 31, No. 8, p. e12992, 2021.
- [29] S. R. Salkuti, “Optimal allocation of DG and D-STATCOM in a distribution system using evolutionary based Bat algorithm”, *International Journal of Advanced Computer Science and Applications*, Vol. 12, No. 4, 2021.
- [30] T. Yuvaraj, K. Ravi, and K. R. Devabalaji, “Optimal allocation of DG and DSTATCOM in radial distribution system using cuckoo search optimization algorithm”, *Modelling and Simulation in Engineering*, Vol. 2017, p. 2857926, 2017.
- [31] S. P. Adam, S. A. Alexandropoulos, P. M. Pardalos, and M. N. Vrahatis, “No free lunch theorem: A review”, *Approximation and Optimization*, Vol. 145, pp. 57-82, 2019.
- [32] L. Wang, Q. Cao, Z. Zhang, S. Mirjalili, and W. Zhao, “Artificial rabbits optimization: A new bio-inspired meta-heuristic algorithm for solving engineering optimization problems”, *Engineering Applications of Artificial Intelligence*, Vol. 114, p. 105082, 2022.

- [33] A. Ulinuha, M. A. Masoum, and S. M. Islam, "Harmonic power flow calculations for a large power system with multiple nonlinear loads using decoupled approach", In: *Proc. of 2007 Australasian Universities Power Engineering Conference*, Perth, WA, Australia, pp. 1-6, 2007.
- [34] S. A. ChithraDevi, L. Lakshminarasimman, and R. Balamurugan, "Stud Krill herd Algorithm for multiple DG placement and sizing in a radial distribution system", *Engineering Science and Technology, an International Journal*, Vol. 20, No. 2, pp. 748-759, 2017.
- [35] D. S. Reddy, V. Janamala, and P. S. Lahari, "Political Optimizer Algorithm for Optimal Location and Sizing of Photovoltaic Distribution Generation in Electrical Distribution Network", *Lecture Notes in Networks and Systems*, Vol. 461, pp. 807-815, 2022.
- [36] D. B. Prakash and C. Lakshminarayana, "Multiple DG placements in distribution system for power loss reduction using PSO algorithm", *Procedia Technology*, Vol. 25, pp. 785-792, 2016.
- [37] S. K. Injeti, "A Pareto optimal approach for allocation of distributed generators in radial distribution systems using improved differential search algorithm", *Journal of Electrical Systems and Information Technology*, Vol. 5, No. 3, pp. 908-927, 2018.
- [38] R. Sanjay, T. Jayabarathi, T. Raghunathan, V. Ramesh, and N. Mithulananthan, "Optimal allocation of distributed generation using hybrid grey wolf optimizer", *IEEE Access*, Vol. 5, pp. 14807-14818, 2017.
- [39] M. G. Hemeida, A. A. Ibrahim, A. A. Mohamed, S. Alkhalaf, and A. M. E. Dine, "Optimal allocation of distributed generators DG based Manta Ray Foraging Optimization algorithm (MRFO)", *Ain Shams Engineering Journal*, Vol. 12, No. 1, pp. 609-619, 2021.
- [40] P. D. Kusuma and A. Dinimaharawati, "Fixed Step Average and Subtraction Based Optimizer", *International Journal of Intelligent Engineering and Systems*, Vol. 15, No. 4, pp. 339-351, 2022.
- [41] P. D. Kusuma and M. Kallista, "Stochastic Komodo Algorithm", *Int. J. Intell. Eng. Syst.*, Vol. 15, No. 4, pp. 156-66, 2022, doi: 10.22266/ijies2022.0831.15.
- [42] F. A. Zeidabadi, S. A. Doumari, M. Dehghani, and O. P. Malik, "MLBO: Mixed Leader Based Optimizer for Solving Optimization Problems", *Int. J. Intell. Eng. Syst.*, Vol. 14, No. 4, pp. 472-479, 2021, doi: 10.22266/ijies2021.0831.41.
- [43] F. A. Zeidabadi, M. Dehghani, and O. P. Malik, "TIMBO: Three Influential Members Based Optimizer", *Int. J. Intell. Eng. Syst.*, Vol. 14, No. 5, pp. 121-128, 2021, doi: 10.22266/ijies2021.1031.12.
- [44] F. A. Zeidabadi, M. Dehghani, and O. P. Malik, "RSLBO: Random Selected Leader Based Optimizer", *Int. J. Intell. Eng. Syst.*, Vol. 14, No. 5, pp. 529-538, 2021, doi: 10.22266/ijies2021.1031.46.
- [45] F. A. Zeidabadi and M. Dehghani, "POA: Puzzle optimization algorithm", *Int. J. Intell. Eng. Syst.*, Vol. 15, No. 1, pp. 273-281, 2022, doi: 10.22266/ijies2022.0228.25.
- [46] S. A. Doumari, H. Givi, M. Dehghani, and O. P. Malik, "Ring toss game-based optimization algorithm for solving various optimization problems", *Int. J. Intell. Eng. Syst.*, Vol. 14, No. 3, pp. 545-554, 2021, doi: 10.22266/ijies2021.0630.46.